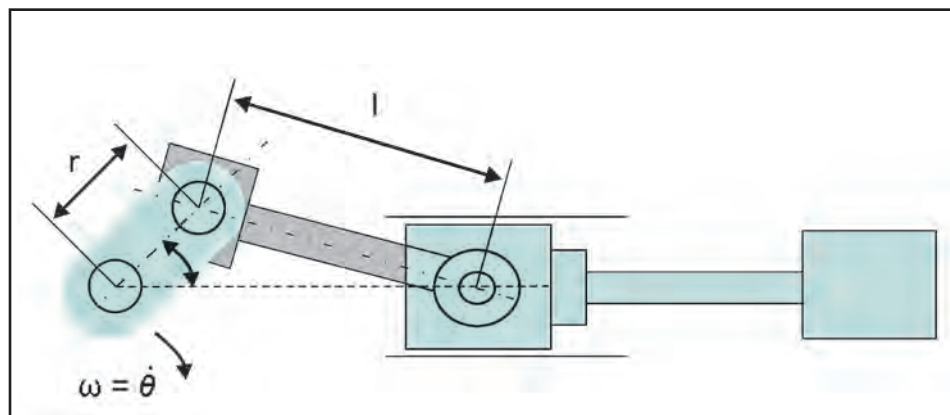




Figure 1. Diagram for calculating gas load on the piston.

Figure 2. Diagram of slider-crank mechanism for determining mass/inertia force.



AN IMPROVED METHOD FOR EVALUATING COMPRESSOR ROD BUSHING DESIGNS

Neuman & Esser Develops New, Field-Validated Approach

By Norm Shade

When designing, selecting and operating reciprocating compressors, the concepts of combined rod load and rod reversal are very important parameters that affect the reliability of connecting rod and crosshead pin bushings. If the combined rod load is too high and/or the rod reversal is too short in duration, then the compressor may suffer a connecting rod (or crosshead pin) bushing failure because of insufficient lubrication. The loss of sufficient lube-oil film thickness allows metal-to-metal contact of the bushing and the crosshead pin.

API Standard 618, "Reciprocating Compressors for Petroleum, Chemical and Gas Industry Services – 4th Edition, June 1995," defines combined rod load as the algebraic sum of the gas load and inertia force. The gas load is the force resulting from the

differential gas pressure acting on the net areas of the piston ends as shown in Figure 1. The inertia force with respect to the crosshead pin is the summation of all the reciprocating masses (piston and rod assembly, crosshead assembly including the pin and any balance weights as shown in Figure 2) times their instantaneous acceleration.

Section 2.4 of API 618 – 4th Edition requires that the combined rod load not exceed the manufacturer's maximum allowable continuous combined rod loading for the compressor running gear at any specified operating load step. These combined rod loads are to be calculated on the basis of the setpoint pressure of the discharge relief valve of each stage and the lowest specified suction pressure corresponding to each load step. For all specified and required operating load steps and the fully unloaded condi-

tion, the component of combined rod loading parallel to the piston rod must fully reverse between the crosshead pin and the bushing during each complete revolution of the crankshaft. It further requires that, unless otherwise specified, the duration of the reversal must be at least 15° of crank angle, and the magnitude of the peak combined reversed load must be at least 3% of the actual combined load in the opposite direction. This reversal is required to maintain proper lubrication between the crosshead pin and bushing.

In the 5th Edition of API 618, the reversal requirement was changed to mandate that the duration and magnitude must be consistent with the oil distribution design of the crosshead bushing in order to maintain proper lubrication. It notes that some bushing designs (e.g., grooved bushings) have

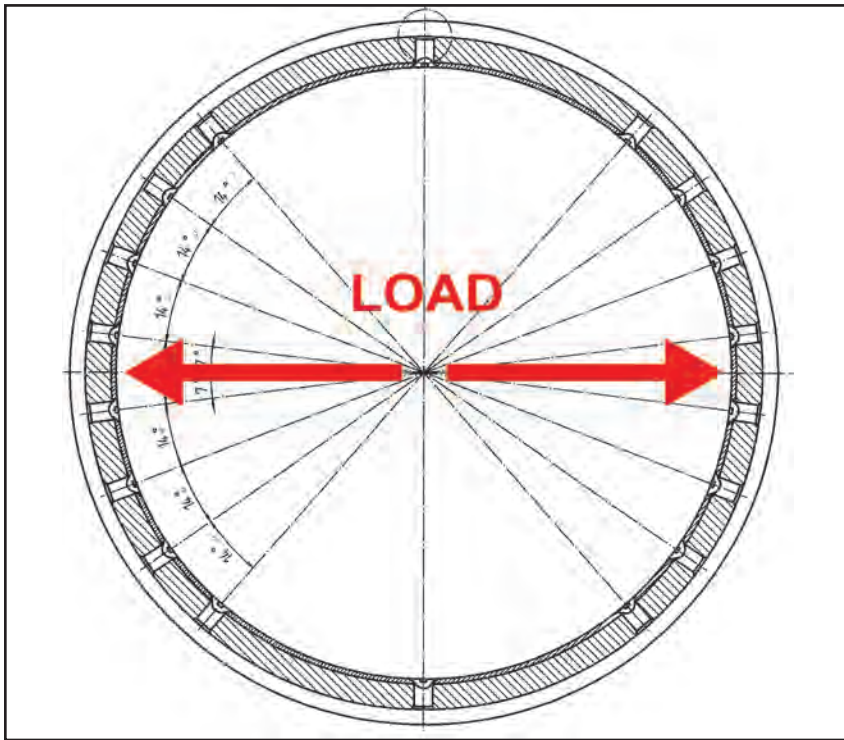


Figure 3. Connecting rod bushing configuration A with multiple oil supply grooves straddling the centerline (in direction of loading).

proven reliability with as little as 15° of rod reversal at 3% load magnitude. However, simple bushing designs (e.g., ungrooved) may require a minimum of 45° degrees of rod reversal and a 20% load magnitude. It says that the manufacturer should provide the actual requirements to the purchaser at the equipment proposal stage.

Compressor manufacturers have various ways of predicting and evaluating the acceptability of pin and bushing loading where lubrication of the surfaces is critical. “Based on the results of our field testing, we were not satisfied that the traditional acceptance standards and calculation procedures were sufficiently dependable in all cases for predicting the acceptable load limits for the connecting rod bushing and crosshead pin,” said Dr. Klaus Hoff, head of central division technology for Neuman & Esser GmbH in Übach-Palenberg, Germany. In an intensive six-month effort, Dr. Hoff developed a new theoretical model that characterizes the lubrication mechanism for connecting rod bushings.

Unlike the main and crank pin bearings of reciprocating compressors, the hydrodynamic working mechanisms of connecting rod bushings and crosshead pins are not so fully understood. The journals of the main and crank pin bearings create hydrodynamic pressure build-up with both rotational and radial movement.

However, the connecting rod bushing can only create hydrodynamic pressure build-up by radial movement. This is the basis for the rod reversal requirement in API Standard 618.

In order to develop an effective algorithm to characterize connecting

rod pin bushing lubrication, Dr. Hoff made a number of simplifying assumptions that are very common in hydrodynamic bearing theory. These included assumptions that both the journal and the bearing are absolutely rigid, i.e., circles remain circles under the load; the bearing axis and journal axis are parallel; the surfaces have no roughness; the oil is a Newtonian fluid, meaning there is no dependency of the oil viscosity on the shear rate; oil flow is laminar; the temperature and, therefore, the viscosity of the oil within the bearing gap, are constant; and the pressure dependency of the oil viscosity is neglected.

A set of complex equations was developed and appropriate boundary conditions were defined. The equations have to be solved for each time step relating to the angular motion of the pin and rod load direction and magnitude. The solution is then repeated until a convergent solution is reached for one revolution of the crankshaft. Although the details of the mathematical model and the numerical solution are beyond the scope of this article, a detailed discussion of them was presented by Dr. Hoff at the 38th Texas A&M Turbomachinery Symposium in September 2009, and the description of the theory can be found in the proceedings of the 6th Conference of the European Forum for Reciprocating Compressors in October 2008.

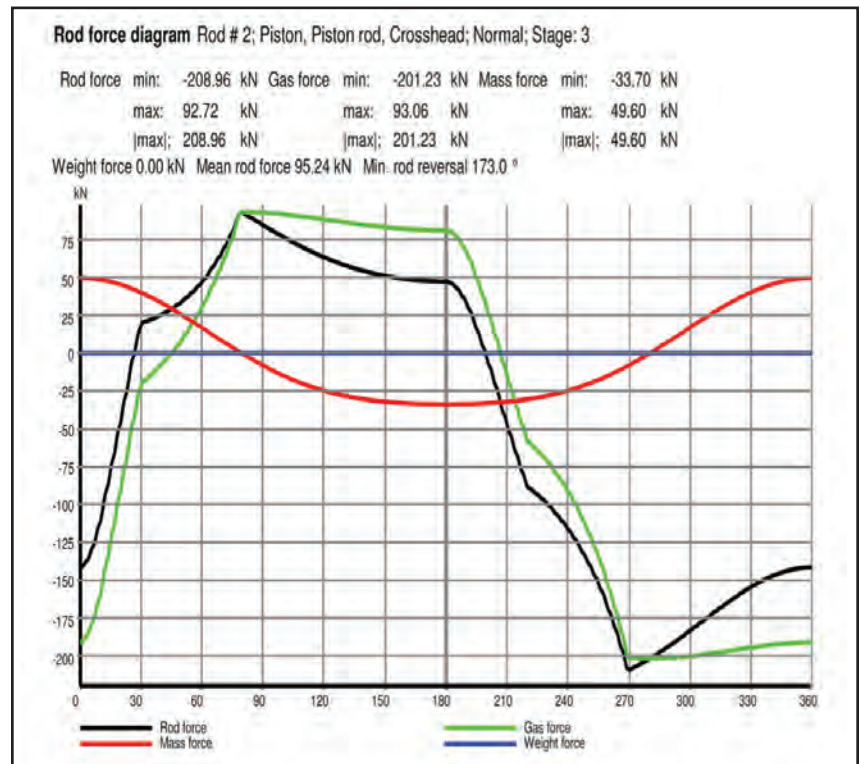


Figure 4. Rod loading for third stage.

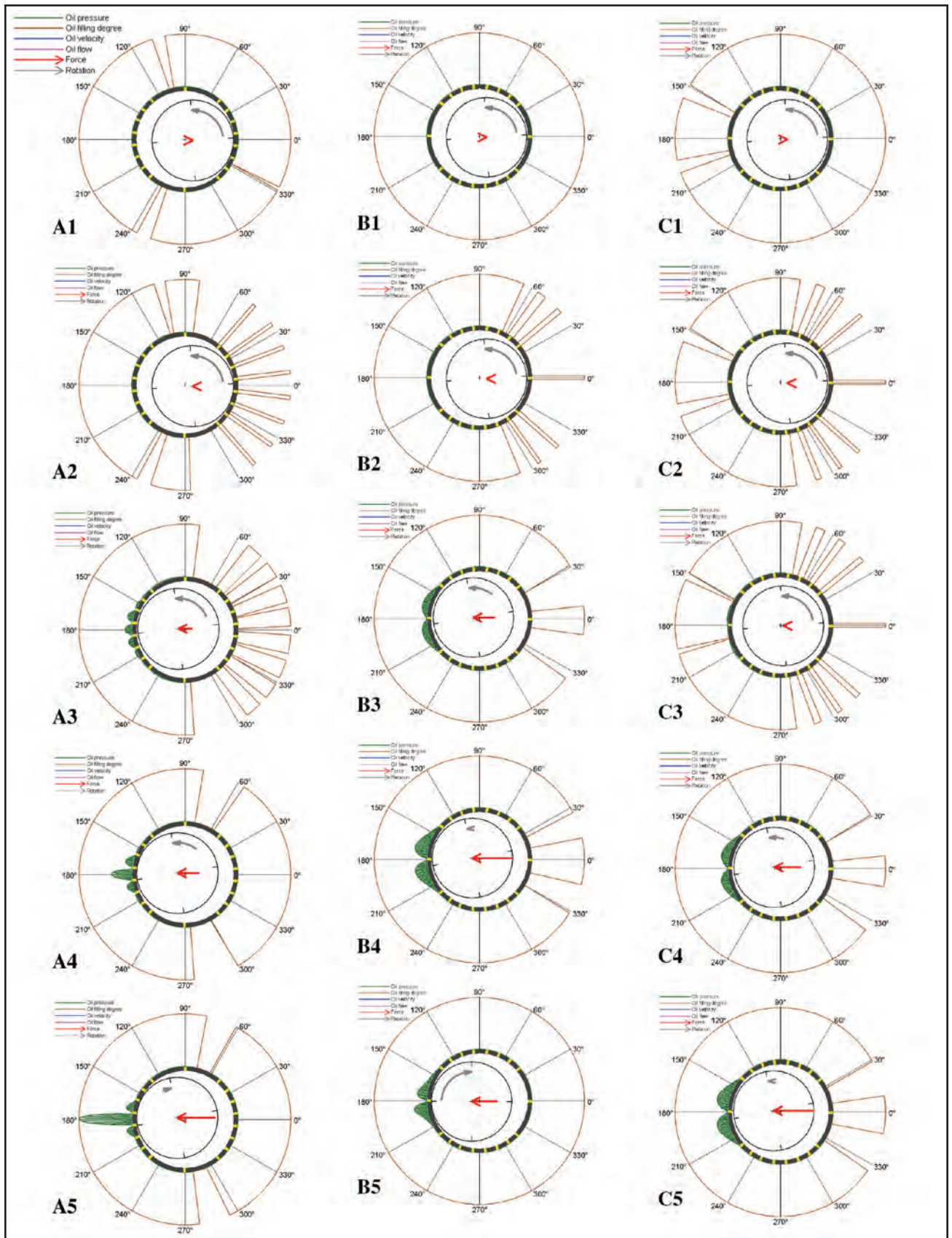


Figure 5a. Calculated results with an oil viscosity of ISO VG 100 for the bushing configuration shown in Figure 3 with multiple grooves straddling the horizontal centerline.

Figure 5b. Calculated results with an oil viscosity of ISO VG 100 for the bushing configuration shown in Figure 7 with a single oil supply groove on the horizontal centerline (in direction of loading).

Figure 5c. Calculated results with an oil viscosity of ISO VG 150 for the bushing configuration shown in Figure 7 with a single oil supply groove on the horizontal centerline (in direction of loading).

With the modeling software, the effects of various design parameters on the connecting rod bushing's load capability can be explored. Neuman & Esser's program revealed some interesting findings about the lubrication of connecting rod bushings and the influence of oil supply grooves and other important parameters. One of the actual compressor configurations that Dr. Hoff used to validate the new modeling software was a Neuman & Esser, four-throw, 1600 hp (1193 kW), 441 rpm, hydrogen makeup compressor operating at a design discharge pressure of approximately 2000 psig (137.9 barg). Several different connecting rod bushing groove configurations were evaluated with the modeling software and compared with actual test observations.

The first case analyzed was bushing configuration A, shown in Figure 3, having multiple grooves straddling the horizontal (direction of piston travel) centerline at 14° intervals. The multiple groove configuration is a common way of directing fresh lubricating oil into the most heavily loaded surfaces of the bearings to carry heat away. Figure 4 shows the calculated rod loading for the third stage of the aforementioned hydrogen makeup compressor.

The analysis explains the influence of the oil supply groove distributions on the hydrodynamic behavior of the crosshead pin bearing. The diagrams in Figure 5a provide a comprehensive summary of the bushing lubrication and loading for the Figure 3 bushing operating in the aforementioned third-stage throw with an oil viscosity of ISO VG 100. Each diagram shows the cross-sectional position of the journal (small inner circle) at a certain time step within the bushing (bigger outer circle). To visualize the movement of the journal, the relative clearance is extremely amplified. The interruptions on the thick circular line of the bushing shell represent the locations of the oil supply grooves in the bushing bore. The central arrow in the journal gives the direction and, by its length, the magnitude of the external rod load. The circular arrow shows the rotational direction and, again by its length, the magnitude of rotational speed. The outer discontinuous line around the bushing shell visualizes the temporary oil-filled or unfilled regions at the inner circumference of the bushing. The shaded parabolic curves between the oil supply grooves show the local oil pressure distribution related to the maximum oil pressure at the displayed time step.

The hydrodynamic situation is visualized at five time steps starting from immediately before the rod load re-



Figure 6. Connecting rod bushing configuration A corresponding to the loading diagrams in Figure 5a, showing heavy wear on the crank-end side after a short period of operation.

versal (crank angle position 200° in Figure 4) to the maximum oil peak pressure (crank angle position 270° or 360°). Diagram A1 shows the situation immediately before the rod load reversal. The important areas of the bushing are filled with oil. Unfilled areas are visible only between 100° and 105° and between 245° and 250°.

Diagram A2 shows the situation immediately after the rod load reversal occurs. Obviously, the oil is completely evaporated in the areas between the oil grooves on that side of the bushing. At time step A3, the journal is already close to the other side of the bushing because of the increasing rod load. The evaporated areas are partly refilled by the oil pre-pressure in the grooves. At time step A4, the vaporized areas are completely filled with oil again and the pressure build-up on the load side of the bushing can be seen. At the maximum load in diagram A5, the maximum pressure situation is reached. An important observation is that only the central load area of the bushing bears the external load by its pressure build-up. The other areas carry minimal load. A remarkable finding of this calculation is that the peak pressure for this bushing configuration is 16.6 times the mean design pressure. An actual test of this bushing in the aforementioned compressor had heavy wear on the crank-end side after a short period of operation as shown in Figure 6, providing a very good validation of the calculations.

Configuration B, shown in Figure 7, is a similar bushing oriented with a single oil supply groove on the horizontal centerline in the direction of loading. Figure 5b shows the calculation results with the same loading as the prior case. The distances to the next oil grooves in the load direction are 41°. The oil viscosity is again ISO VG 100. Diagram B1 shows the situation immediately before the rod load

reversal. Unlike the earlier orientation in diagram A1, the entire bushing is filled with oil. B2 shows the situation immediately after the rod load reversal. Again, the oil is completely evaporated in the areas between the oil grooves on that side of the bushing. At time step B3, the journal is already close to the other side of the bushing because of the increasing rod load. The evaporated areas are partly refilled again by the oil pre-pressure in the grooves, but more time for the refilling is needed because of the longer distance between the grooves. At time step B4, a further pressure build-up is visible because of the highest rod load at this time step. The refilling of the unloaded side progresses, but is not finished yet. Time step B5 shows the situation at maximum oil peak pressure. Two pressure parabolas bear the external load. This groove orientation reduces the maximum peak pressure to only 4.3 times the mean design pressure. This is the result of approximately two 41° areas being loaded in configuration B instead of only one 14° degree section in configuration A.

Figure 5c shows the calculation results for configuration C, which is the same bushing configuration as B in Figure 7, except that the oil viscosity is ISO VG 150 instead of 100. Diagram C1 shows the situation immediately before the rod load reversal. Unlike configuration B, the unloaded bushing side is not yet completely filled with oil. Diagram C2 illustrates the situation immediately after the rod load reversal. Again, the oil is completely evaporated in the areas between the oil grooves on that side of the bushing.

At time step C3, the journal is moving to the other side of the bushing because of the increasing rod load. This rapid movement supports the refilling of the now loaded area. The refilling of the loaded area is finished before the maximum load occurs. The evaporated areas on the unloaded side are partly refilled again by the oil pre-pressure in the grooves, but more time for the refilling is needed because of the longer distance between the grooves and the higher viscosity.

At time step C4, a further pressure build-up is visible because of the higher rod load at this time step; the refilling at this loaded side is done and the refilling of the unloaded side progresses, but is not yet finished. Time step C5 shows the situation at maximum oil peak pressure. In this case, it is also the time step with the maximum load. Two pressure parabolo-

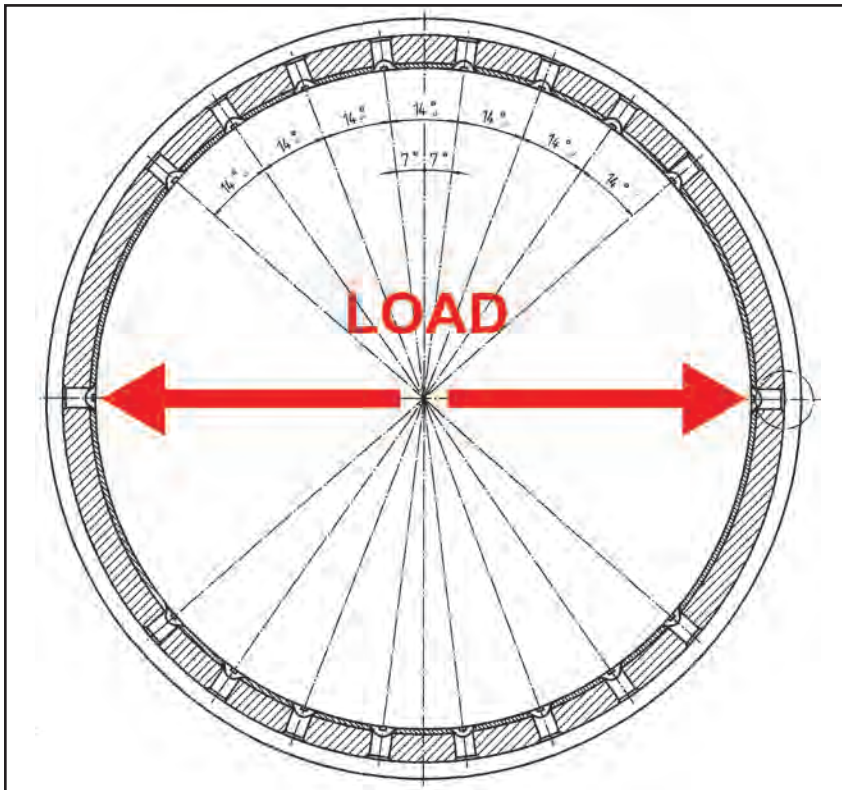


Figure 7. Connecting rod bushing configurations B and C oriented with a single oil supply groove on the horizontal centerline (in direction of loading).

las bear the external load, and the ratio of the peak pressure to the mean pressure is further improved to 4.0. The more important improvement between configurations C and B is the increase of the minimum oil film thickness to 0.11 mil from 0.07 mil (2.9 μm from 1.9 μm). An actual test of this bushing in the aforementioned compressor indicated no wear after a long period of operation as shown in Figure 8, which was a good validation of the computations.

“The bushing pattern in configuration A shows that failure was occurring because of excessive wear, the improvement of the minimum oil film thickness by these measures provided a much better arrangement that avoids the wear problem,” said Hoff.

Neuman & Esser used the new hydrodynamic design program for a parametric study of several compressor applications, including the aforementioned unit, to establish empirical acceptance criteria. A key factor in the evaluation is the comparison of the minimum calculated oil film thickness with the critical film thickness (at which metal-to-metal contact occurs). However, Hoff found that this relationship is only valid when the refilling of the bushing is reached on each reversal.

A second criterion was developed to assess the refilling of the bushing,

which is a function of the rod load distribution and the bearing design parameters. The calculated value of a given load scenario and bearing design must exceed a critical limit, which depends on the bearing design. This refilling characteristic is much more complex and accurate than the minimum rod load reversal criterion given in API 618, for example. Defining only a minimum rod load reversal angle and a corresponding peak load can be either critical or conservative since these parameters do not fully describe the refilling mechanism. The refilling characteristic contains all variables influencing the refilling.

“Our calculations and test results

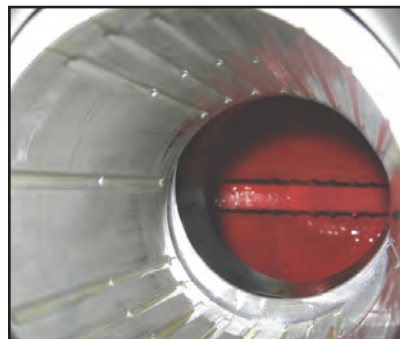


Figure 8. Connecting rod bushing configuration B corresponding to the loading diagrams in Figure 5b, showing no indication of wear after a period of operation.

showed that a tremendous upgrade of a bushing can be obtained just by rearranging the oil supply grooves and increasing the oil viscosity. In doing so, the evaporation of the oil caused by the fast movement of the journal between the load land areas of the bushing is a critical phenomenon that must be known and taken into account. These areas of evaporated oil need to be refilled with fresh oil from the oil supply grooves. This can become critical for load cases with a small angle of rod load reversal and relatively large angle between the oil supply grooves. In such a case, where the refilling cannot be accomplished, the bearing can fail because of lack of lubrication. The bushing failure pattern from inadequate refilling is similar to the pattern of a bushing failure resulting from a load without rod load reversal,” explained Hoff.

“Our computational method is able to predict the hydrodynamic oil pressure distribution, including the peak pressure, the journal eccentricity and, therefore, also the minimum oil film thickness on the basis of the given assumptions. In addition, a correct prediction of the evaporation and refilling process is included. With this tool, a reliable connecting rod bushing design is possible,” he added. Hoff went on to say that from this work, three design criteria need to be taken into account for a reliable connecting rod bushing design: 1. the hydrodynamic oil peak pressure must not exceed a critical value to avoid a bearing fatigue failure; 2. the minimum hydrodynamic oil film thickness must not fall below a critical value to avoid a bearing failure from lack of lubrication; 3. the rod load reversal, defined by a newly introduced refilling characteristic, must exceed a critical value to avoid bushing damage caused by lack of lubrication from inadequate refilling.

“Defining a limit for the reversal angle and the peak load can be risky. The time for refilling loaded areas of the bushing with fresh oil must be adequate. This might be adequate with as little as 10° of reversal, but in other cases, it might not be adequate with 50°. Unfortunately, design measures that improve the situation concerning criteria 1 and 2 cause a deterioration of criterion 3. We can now check for peak pressure, minimum oil film thickness, and the time for refilling, as well as the critically important relationship between them. From this, we have developed screening functions to determine acceptability, and we can then further analyze any marginal cases. The design task is to find the optimum compromise,” concluded Dr. Hoff. ©